CONSTITUTIVE MODELLING OF A TIRE PLUNGER TEST THROUGH FINITE ELEMENT SIMULATION

William Manjud Maluf Filho

wmaluf@fei.edu.br

Mechanical Engineering Department of Centro Universitário da FEI

3972-B Humberto de Alencar Castelo Branco Ave, São Bernardo do Campo, SP 09850-901, Brazil

Automotive Engineering Center of Escola Politécnica da Universidade de São Paulo (CEA Poli-USP)

2231, Prof. Mello Moraes Ave, São Paulo, SP 05508-030, Brazil

Debora Francisco Lalo

Marcelo Greco

debora@dees.ufmg.br

mgreco@dees.ufmg.br

Federal University of Minas Gerais

6627 Antônio Carlos Ave, building 1, Department of Structural Engineering - 4th floor, Belo Horizonte, MG 31270-901, Brazil

Abstract. *Almost all road vehicles have wheels with pneumatic tires. Tire development made possible to the automotive industry to design comfortable and safe road vehicles. According to the Federal Motor Vehicle Safety Standards (FMVSS) some test procedures for tire endurance, high-speed performance and strength are required. Tire strength, for example, is verified by a Plunger Test. This test procedure aims to press the tire by a cylindrical steel plunger with a hemispherical end perpendicularly into a raised tread element as near as possible to the centerline of the tread, at a rate of 50 mm/min, until the tire breaks or the plunger is stopped by the rim. Thus, the Plunger test is performed to determine the belts breaking energy value for the tire. These values are taken into account to estimate the tire reliability. Due to the physical nonlinearity and uncertainty inherent in tire system a three-dimensional finite element model (FEM) was proposed. The elastomers were modeled by*

Proceedings of the XXXVIII Iberian Latin-American Congress on Computational Methods in Engineering P.O. Faria, R.H. Lopez, L.F.F. Miguel, W.J.S. Gomes, M. Noronha (Editores), ABMEC, Florianópolis, SC, Brazil, November 5-8, 2017.

using the Mooney-Rivilin model and the composites by the equivalent orthotropic material model based on the Halpin-Tsai equations in the commercial software Abaqus®. The hyperelastic material constants were obtained from experimental data and are confidential for the tire industry. Comparisons between numerical and experimental Plunger test results demonstrated the accuracy of the proposed model where numerical results presented errors less than 10%.

Keywords: *Plunger test, Hyperelastic constitutive model, Finite element analysis*

1 TIRE CHARACTERIZATION

Wheels have been discovered centuries ago. The tire's invention, and further enhancement, made it possible to the automotive industry engineers to design comfortable and safe road vehicles.

Tires are supposed to fulfill the following functions: support vehicle weight, properly absorb forces (Wong, 2008), provide vibration damping, cushion the vehicle over surface irregularities (Dai Vu et al., 2017; Matsubara et al., 2017), contribute to cornering stability providing adequate steering control (Wang & Wang, 2013), provide sufficient traction for driving and braking in different surfaces, grant operational safety (Ružinskas & Sivilevičius, 2017). To fulfill these functions properly, tires are required to have some characteristics such as: having low rolling resistance, minimally heat up, rolling noise reduction (Hoever & Kropp, 2015), present excellent adhesion on wet surfaces (Xie et al., 2016) and display maximum fatigue life (Schön et al., 2014; Diaz et al. 2016).

The main objective of air pressure inside the tire is to enhance its structural stiffness (Cueto et al., 2016). The air pressure "p_a" causes sidewalls bending. The normal forces "F_a" are applied in the bead area and the outcome on the rim is a vertical load "F_z". The forces carried by a tire and the moving reference system $S = (x, y, z; O)$ are depicted in Fig. 1.

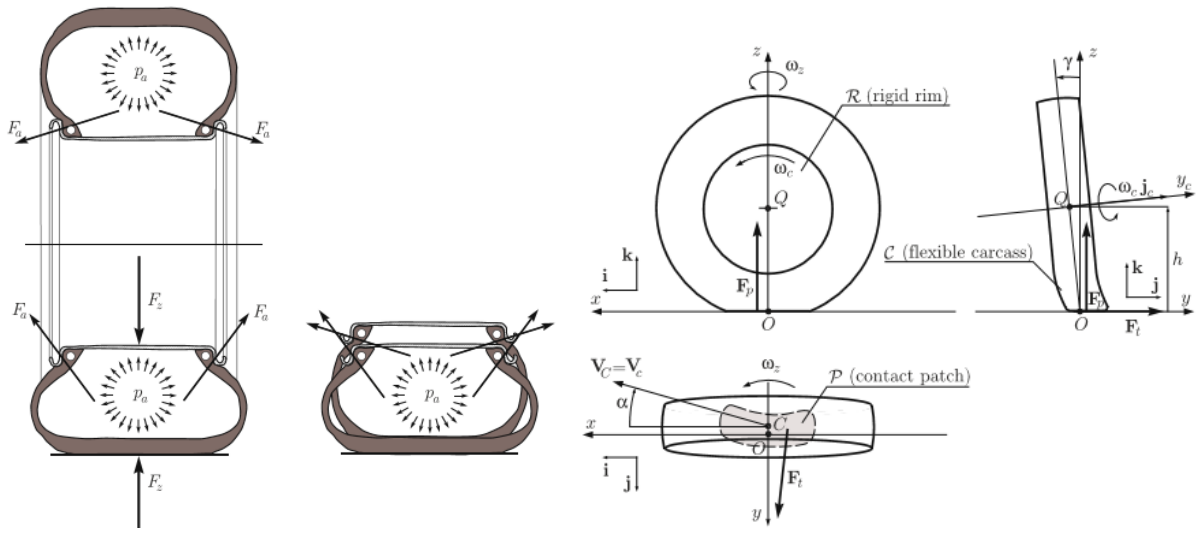

Figure 1. Tire loads and vehicle moving reference system (Guiggiani, 2014)

Most of the forces and moments influencing the motion of a ground vehicle, aside from aerodynamic and gravitational forces are applied through the tire–ground contact (Xiong &

Tuononen, 2015). In a classic work, Gillespie (1992) affirmed that tire and vehicle interaction are a very complex matter. Tire characterization and suspension simulation play an important role in vehicle dynamics (Winroth, et al., 2017).

According to Faroni (2016) the vehicle degrees of freedom (DOF) need to be considered. In particular, DOF should refer to in plane vehicle body motions (longitudinal, lateral and yaw motions), wheel rotations and wheel steering angle (Abdolmaleki et al., 2015). In order to illustrate the complexity of this matter, the data necessary for a simple vehicle characterization are shown in Table 1.

Table 1. Summary of vehicle and tire characterization parameters (Faroni, 2016)

Vehicle data	Symbol	Unit
Sidewall markings of the front tire to be characterized		
Sidewall markings of the rear tire to be characterized		
Front tire unloaded radius	R_{0F}	[m]
Rear tire unloaded radius	R_{0R}	[m]
Front tire effective rolling radius	R_{rF}	[m]
Rear tire effective rolling radius	R_{rR}	[m]
Dry vehicle mass	m	[kg]
Liquids mass-full tanks	M_L	[kg]
Front wheel+tire mass	M_{wF}	[kg]
Rear wheel+tire mass	M_{wR}	[kg]
Vehicle moment of inertia about *z*-axis	J_z	[kg m^2]
Front wheel moment of inertia about rotation axis	I_{wF}	[kg m^2]
Rear wheel moment of inertia about rotation axis	I_{wR}	[kg m^2]
Wheelbase	l	[m]
Front wheelbase	a	[m]
Rear wheelbase	b	[m]
Front track	t_F	[m]
Rear track	t_R	[m]
Center of gravity height	h	[m]
Front axle roll stiffness	$K_{\Phi F}$	[N/rad]
Rear axle roll stiffness	$K_{\Phi R}$	[N/rad]
Nominal steering ratio	τ_s	[−]
Vehicle master section	A_v	[m^2]
Cx	C_x	[−]
Cz front	C_{zF}	[−]
Cz rear	C_{zR}	[−]
Roll center height at center of gravity abscissa	d	[m]
Roll center height at font axle abscissa	d_F	[m]
Roll center height at rear axle abscissa	d_R	[m]
Static camber angle front	γ_{0F}	[rad]
Static camber angle rear	γ_{0R}	[rad]
Static toe angle front	χ_{0F}	[rad]
Static toe angle rear	χ_{0R}	[rad]
Real/geometric maximum available Ackermann angle	ack%	[−]
Datron distances from CG (*x*, *y*, *z*)	b_x, b_y, b_z	[m, m, m]
Rolling resistance curves		
Elasto-kinematic suspensions characterization		
Axle compliances characterization		

Besides the interaction of rolling tire and vehicle, it is also important to consider the road surface skid resistance (Sun et al., 2017) and mechanical responses of soil materials (Recuero, et al., 2017) that are subjected to cyclic loading. Additionally, the inelastic ground deformation and frictional sliding phenomena, induced by vehicle's movement must be taken into account (Zhao & Zang, 2017; Ozaki & Kondo, 2016).

2 TIRE TEST PROCEDURES

The National Highway Traffic Safety Administration (NHTSA) is an agency of the Executive Branch of the U.S. government, part of the Department of Transportation (DOT), which issues Federal Motor Vehicle Safety Standards (FMVSS). The FMVSS are U.S. federal regulations specifying design, construction, performance, and durability requirements for motor vehicles and regulated automobile safety-related components, systems, and design features.

FMVSS No. 119 is a standard that establishes performance and marking requirements for tires for use on multipurpose passenger vehicles, trucks, buses, trailers, and motorcycles. This standard specifies test procedures for tire endurance, high-speed performance and strength.

Tire strength is verified by the plunger test. Test procedure aims to force a cylindrical steel plunger with a hemispherical end. The diameter is specified according to the tire size, pressing the tire perpendicularly into a raised tread element as near as possible to the centerline of the tread, at a rate of 50 mm/min ($8.3x10^{-4}$ m/s), until the tire breaks or the plunger is stopped by the rim.

The Plunger test is performed to determine the belts breaking energy value for the tire according to ASTM F414-06 (2006) standard test method. This standard accounts for the energy absorbed by a tire when deformed by slow-moving plunger in order to estimate the tire reliability. The test method specifies the tire plunger energy required to completely penetrate the tread area of an inflated tire as indicated by a rupture, loss of inflation pressure, sudden drop in plunger force or bottom-out. For the test implementation it is required a laboratory testing machine capable of slowly penetrating the tire tread surface with a cylindrical plunger. A typical testing system is depicted in Fig. 2.

Figure 2. Tire strength testing system (Harris & Evans, 2013)

Test procedure includes preparation of the tire as per ASTM F414-06 (2006) standard, including mounting the tire and inflating it until a specified pressure. The tire is then, conditioned at a room temperature for at least 3h. Then, tire pressure is adjusted to the specified test pressure based on the maximum pressure listed on the sidewall. Afterwards, the test is conducted as mentioned previously.

It is very important to avoid penetration into the tread groove. The load “F” and deflection “δ” are recorded for the 5 test points equally spaced around the circumference of the tire.

If the tire fails to break before the plunger is stopped by reaching the rim, the force and penetration as the rim is reached is recorded and used to calculate the energy for each test point. The strength energy is calculated by Eq. (1).

$$W = \frac{F \cdot \delta}{2} \quad (1)$$

For instance, a tire 325/35R28 was tested and reported by Harris & Evans (2013). The obtained load vs deflection graph is depicted in Fig. 3. According to the standard FMVSS No. 109 the minimum breaking energy for this tire is 5200 lbf.in. The maximum plunger penetration was 5.17 inches under a load of 3257 lbf. The maximum strength energy for the tested tire was 8418 lbf.in exceeding the minimum energy specified.

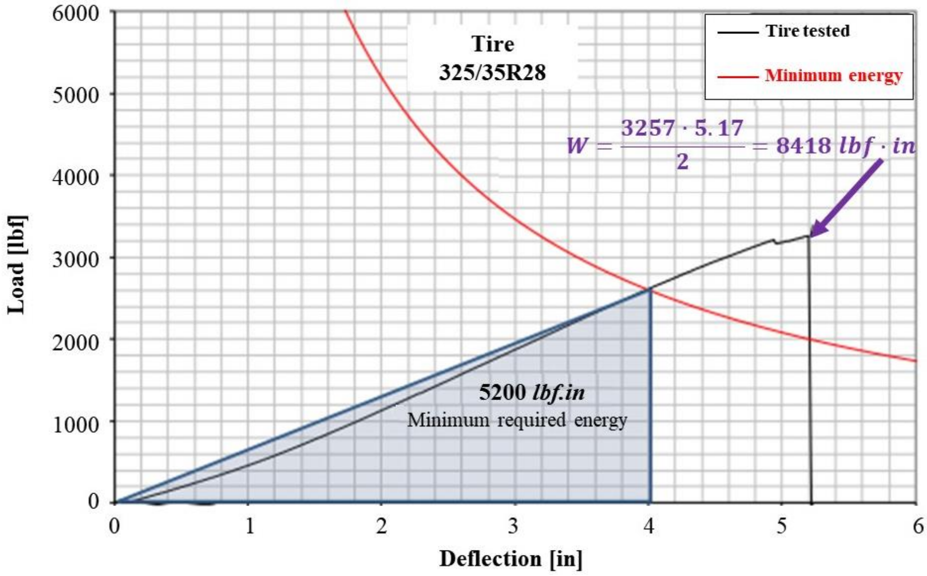

Figure 3. Load vs deflection graph of a tire 325/35R28 (Adapted from Harris & Evans, 2013)

3 HYPERELASTIC CONSTITUTIVE MODELING

Testing data are commonly used to calibrate constitutive models (Montella et al. 2014). This is especially important in FEM simulations, once rubber-like materials exhibit an intricate nonlinear performance. Due to the macromolecular network structure of rubber-like materials, a stress-strain behavior (primarily governed by changes in configurational entropy) is a result of randomly-oriented molecules that become preferentially-oriented during stretching (Chen et al. 2017). Effects such as hysteresis, viscoelasticity and stress softening phenomenon play an important role in rubber behavior (Khajehsaeid et al. 2014; Marckmann et al. 2016). The last case calls Mullins effect and occurs during the first cycles of loading (Mullins, 1969).

Large-strain elasticity applied to hyperelastic isotropic and incompressible materials models are based on the definition of a strain-energy function "W" (Sasso et al. 2008). This strain energy is expressed as a function of the strain tensor invariants or principal stretches, as in Eq. (2).

$$W = W(I_1, I_2, I_3) = W(\lambda_1, \lambda_2, \lambda_3) \quad (2)$$

The strain tensor invariants are described as a function of the principle extension ratios λ_1, λ_2 and λ_3 described by Eq. (3).

$$\begin{cases} I_1 = \lambda_1^2 + \lambda_2^2 + \lambda_3^2 \\ I_2 = (\lambda_1\lambda_2)^2 + (\lambda_2\lambda_3)^2 + (\lambda_1\lambda_3)^2 \\ I_3 = (\lambda_1\lambda_2\lambda_3)^2 \end{cases} \tag{3}$$

Incompressible materials have the third invariant (I_3) equal to one. This results in strain-energy function that will depend only on I_1 and I_2. In continuum mechanics the most common constitutive models used to represent hyperelastic materials are: Mooney–Rivlin, Ogden, Arruda–Boyce, Yeoh and Neo-Hookean (Bergstrom, 2015).

3.1 Mooney–Rivlin

Mooney (1940) postulated that: “if a material is isotropic, if its hysteresis and volume change are negligible and the shear is proportional to the traction in simple shear in a plane previously deformed, if at all, only by uniform dilatation or contraction”, then the general strain-energy function could be described by Eq. (4).

$$W = \frac{G}{4}\sum_{i=1}^{3}\left(\lambda_\mathrm{i} - \frac{1}{\lambda_\mathrm{i}}\right)^2 + \frac{H}{4}\sum_{i=1}^{3}\left(\lambda_\mathrm{i}^2 - \frac{1}{\lambda_\mathrm{i}^2}\right) \tag{4}$$

When the author originally proposed the model, it was established that λ_i were the principal stretches, G the shear modulus, and H was a new elastic constant not found in previous theories.

According to Rivlin (1948) “the equations of motion, boundary conditions and stress-strain relations for a highly elastic material can be expressed in terms of the stored-energy function”. So the Mooney model was expressed in terms of invariants. The first order Mooney-Rivlin model is presented by Eq. (5).

$$W = C_{10}(I_1 - 3) + C_{01}(I_2 - 3) \tag{5}$$

where, C_{ij} are material constants obtained from testing data (Soares & Gonçalves, 2014). Thus, it is possible to expand Eq. (5) to the second order terms as per Eq. (6).

$$W = C_{10}(I_1 - 3) + C_{01}(I_2 - 3) + C_{20}(I_1 - 3)^2 + C_{11}(I_1 - 3)(I_2 - 3) + C_{02}(I_2 - 3)^2 \tag{6}$$

Equation (6) represents the strain-energy density function dependence on other material parameters. It is useful to describe stress-strain response at higher strain levels (Cheviakov & Ganghoffer, 2012).

3.2 Ogden

Ogden (1972) presented the correlation of theory and experiment for incompressible isotropic elastic solids under isothermal conditions and finite strain. The strain energy function is presented by Eq. (7).

$$W(\lambda_1, \lambda_2, \lambda_3) = \sum_{p=1}^{N} \frac{\mu_\mathrm{p}\left(\lambda_1^{\alpha_p} + \lambda_2^{\alpha_p} + \lambda_3^{\alpha_p} - 3\right)}{\alpha_p} \tag{7}$$

Proceedings of the XXXVIII Iberian Latin-American Congress on Computational Methods in Engineering
P.O. Faria, R.H. Lopez, L.F.F. Miguel, W.J.S. Gomes, M. Noronha (Editores), ABMEC, Florianópolis, SC, Brazil, November 5-8, 2017.

According to Ogden (1997; 2007), N is a positive integer assumed to be 3 (but can be larger or even smaller), α_p and μ_p are real algebraic parameters that satisfy the condition expressed by Eq. (8).

$$\mu = \frac{1}{2}\sum_{p=1}^{N} \mu_p \alpha_p \quad (8)$$

where μ is the ground state shear modulus.

Analyzing Eq. (7) it is possible to demonstrate that for $\alpha_1 = 2$ and $\alpha_2 = -2$, it is equivalent to the first order Mooney-Rivlin function with $C_{10} = 0{,}5\mu_1$ and $C_{01} = -0{,}5\mu_2$.

3.3 Arruda–Boyce

Statistical and continuum mechanics approaches were incorporated by Arruda & Boyce (1993). Authors have shown that higher order continuum mechanics models are accurate since they describe the physics of successful non-Gaussian statistics models. So, they adequately provide relation between the higher order continuum models and the statistical mechanics models. The Arruda-Boyce model, based on assigned coefficients "C_i", is expressed in Eq. (9).

$$W = \mu \sum_{i=1}^{5} \frac{C_i}{\lambda_m^{2i-2}} \left(I_1^i - 3^i\right) \quad (9)$$

where λ_m is the limiting network stretch and the material parameter μ is defined as Eq. (10).

$$\mu = n.k.\Theta \quad (10)$$

in which "n" is the chain density, "k" is the Boltzmann's constant, and "Θ" the temperature.

3.4 Neo-Hookean

Treloar (1946) have proposed the neo-Hookean model based on I_1 as a material parameter. The model is expressed in Eq. (11).

$$W = C_{10}(I_1 - 3) \quad (11)$$

3.5 Yeoh

Yeoh (1993) proposed a model that accounts for the principal features of swollen rubber. Unlike Mooney-Rivlin and neo-Hookean models, Yeoh model is applicable over a wide range of strains. The model is expressed in Eq. (12).

$$W = \sum_{i=1}^{3} C_{i0}(I_1 - 3)^i \quad (12)$$

4 HALPIN-TSAI MODEL COMPOSITE CONSTITUTIVE MODELING

Acording to Shokrieh & Moshrefzadeh-Sani (2016) it is very well accepted to predict elasticity of composite material using Halpin-Tsai model. The mathematical model is a technique to calculate the stiffness of composites reinforced by micro and nano particles. It is based on the geometry and orientation of the filler and the elastic properties of the filler and matrix.

In this method, first the longitudinal and transverse moduli of composites are calculated. Then, the elastic modulus of randomly oriented composites is obtained using an equation containing a constant coefficient. This coefficient is assumed to be constant and independent of the matrix and reinforcement properties (Halpin & Kardos, 1976). The model is based on the Hartree–Fock, also called self-consistent field method (Pavarini et al., 2016).

According to Mouritz & Gibson (2007) the Halpin-Tsai general form is expressed in Eq. (16).

$$P = HS\left(P_f, P_m, V_f, \xi_p\right) = P_m \frac{1+\xi_p \eta_p V_f}{1-\eta_p V_f} \quad \text{where } \eta_p = \frac{P_f - P_m}{P_f + \xi_p P_m} \tag{16}$$

"HS" is a function that represents the Halpin-Tsai relationship. P_f and P_m are the equivalent fiber and matrix values, respectively, of the property in question. The "ξ_p" is the factor that relates the influence of the phase arrangement for the particular property.

5 FINITE ELEMENT SIMULATION

Modeling tires geometry and their behavior are very complex engineering. Loading conditions, which can be quasi-static or dynamic, are also affected by severe contact restrictions (Cueto et al. 2013).

Abe (2015) presented a theoretical investigation into the effects of tire parameters on vehicle's dynamics. Typically, authors based their analysis on the classical mathematical model presented by Fiala (1954). A common tire structural model is depicted in Fig. 4.

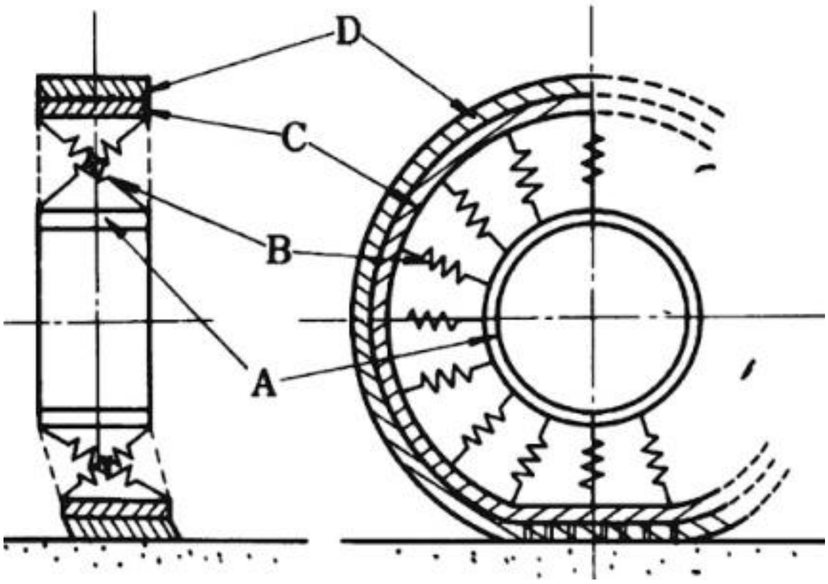

Figure 4. Tire structural model (Abe, 2015)

Although the models seem to be simple, tire manufacturing is a highly complex process (Gupta et al., 2017) consisting of four major steps, including mixing, component preparation, building, and curing (Kim et al., 2017). According to Choi & Lyu (2017) automotive tires start mixing crude rubber with carbon black and sulfur to form a rubber with desirable elastic properties. Extrusion process follows to produce rubber layers that will form a cylindrical green tire. Lastly it undergoes vulcanization and due to the curing process it becomes a structure with a balanced elasticity and rigidity. During the curing process, high-pressure steam is applied to the bladder, forcing the green tire to expand onto the mold. This will lead to adopting its shape and forming a tire with unique and complex groove on the tread region.

Tire construction methods vary somewhat in the number and type of components. Tire carcass is composed by the tread, bead, sidewall, shoulder, and ply. Important constituents such as (1) tread, (2) sidewall, (3) rim, (4) fabric airbag, (5)–(8) radial cords, (9) circumferential cords are depicted in Fig. 5.

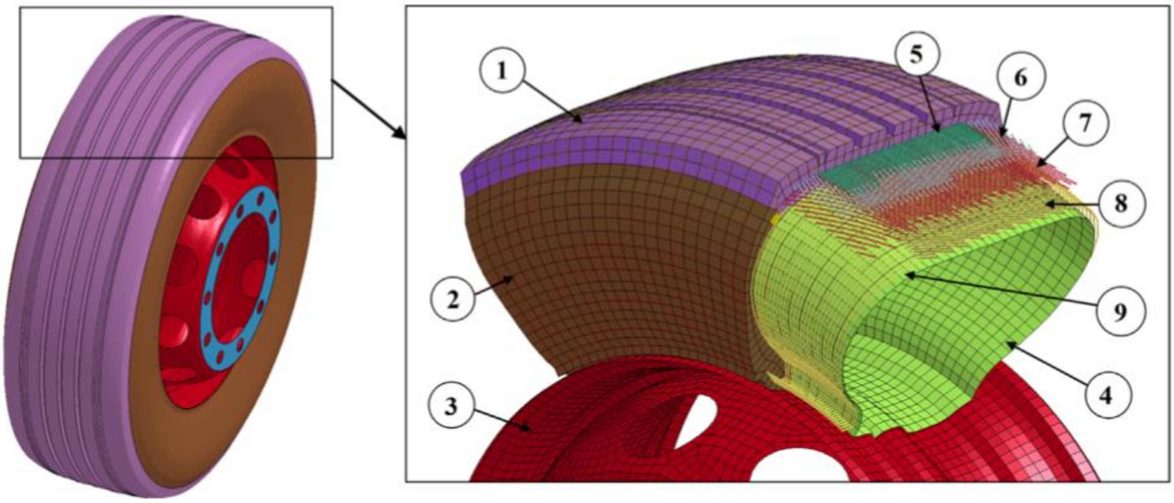

Figure 5. Rim and tire components (Baranowski et al., 2016)

Tires are elaborated engineered components since they are a conglomerate of 3 completely contrasting materials: metals, polymers and composites (Jia et al., 2017).

Polymers such as rubber have high elasticity, low density, long service life, light weight and relatively low cost (Lijuan et al., 2014). The macrostructure and the glass transition temperature have a dominant role in wear resistance (Kern & Futamura, 1988).

Tire composites are a network of fiber/textile/steel cord structures arranged in a parallel configuration and imbedded in a rubber matrix (Kersker et al, 1969). Cords should present high modulus and low shrinkage characteristics as well as excellent dimensional stability. It is also desired to have retention of relaxation modulus under constant strain and to exhibit greater elasticity at room temperature (Tonatto et al., 2017).

The finite element model was implemented in the Abaqus® commercial software. This software is extensively applied to perform tire structural analysis as it can be found in works published by Costa (2000), Maluf Filho (2002), Costa (2007), Neves et al. (2008), Chang & Yang (2009), Liu et al. (2010), Xia (2011), Behroozi et al. (2012), Kuster et al. (2013), Tang et al. (2014), Cho et al. (2015), Wei & Olatunbosun (2016) and Rafei et al. (2017).

The plunger test is a dynamic experiment. Nevertheless, in this paper we propose to model it by means of a quasi-static analysis. In a classic study on the dynamic axial response

Proceedings of the XXXVIII Iberian Latin-American Congress on Computational Methods in Engineering
P.O. Faria, R.H. Lopez, L.F.F. Miguel, W.J.S. Gomes, M. Noronha (Editores), ABMEC, Florianópolis, SC, Brazil, November 5-8, 2017.

of idealized elastic–plastic models, rods, cylindrical shells and square tubes, Jones (2003) discussed the dynamic plastic instability of structural members, subjected to large axial impact loads. The author has shown that quasi-static methods of analysis can be applied correctly when the striking mass is much larger than the mass of the rod and the velocity impact is lower than 15 m/s.

A tridimensional non-linear model based on the Mooney-Rivlin and Halpin-Tsai hyperelastic constitutive equations was used in finite element simulation. The 3D model of a truch tire is depicted in Fig. 6. Different colors refer to different tire components with different material properties. Parameters were obtained by experimental testing. In this figure, "R" stands for components made of rubber; "S" relates to steel; and "C", composites.

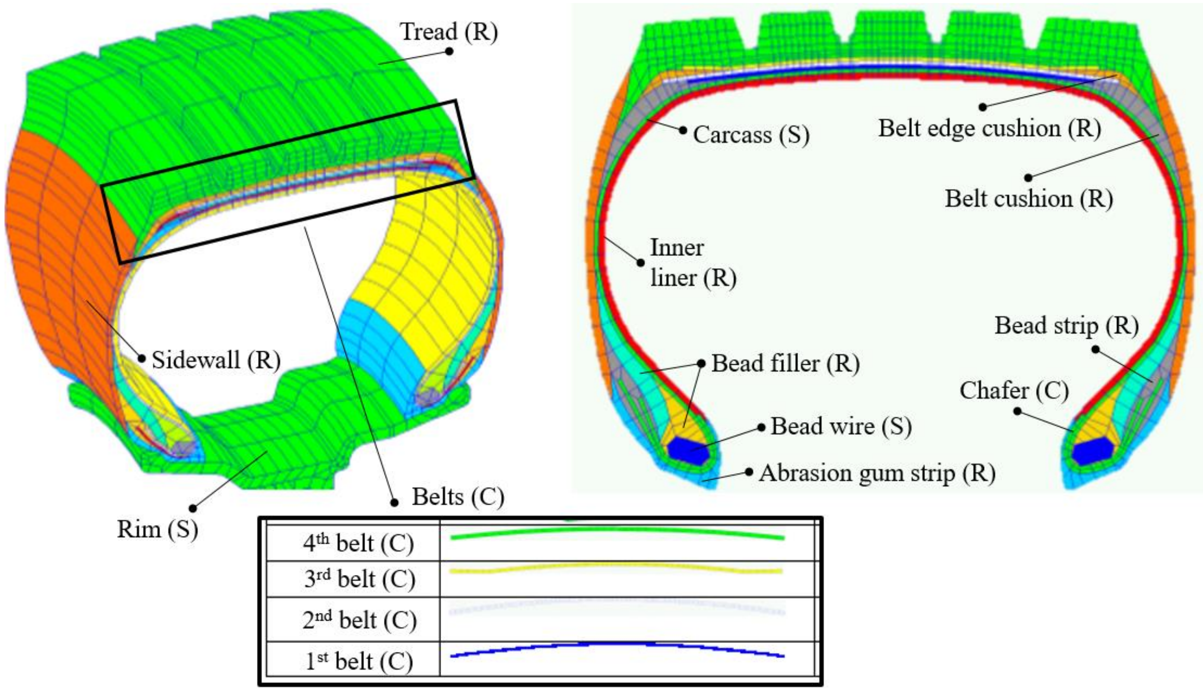

Figure 6. 3D finite element model used to describe a tire

The rubber parts were modeled with 50000 C3D8H elements. The letter H represents a hybrid formulation, thus the hydrostatic stress component can be treated as an independent variable, avoiding volumetric locking. Approximately 331000 DOFs were taken into account in during 145h simulation. The composites were modeled using the Abaqus Rebar element (Simulia, 2016) as it is depicted in Fig. 7.

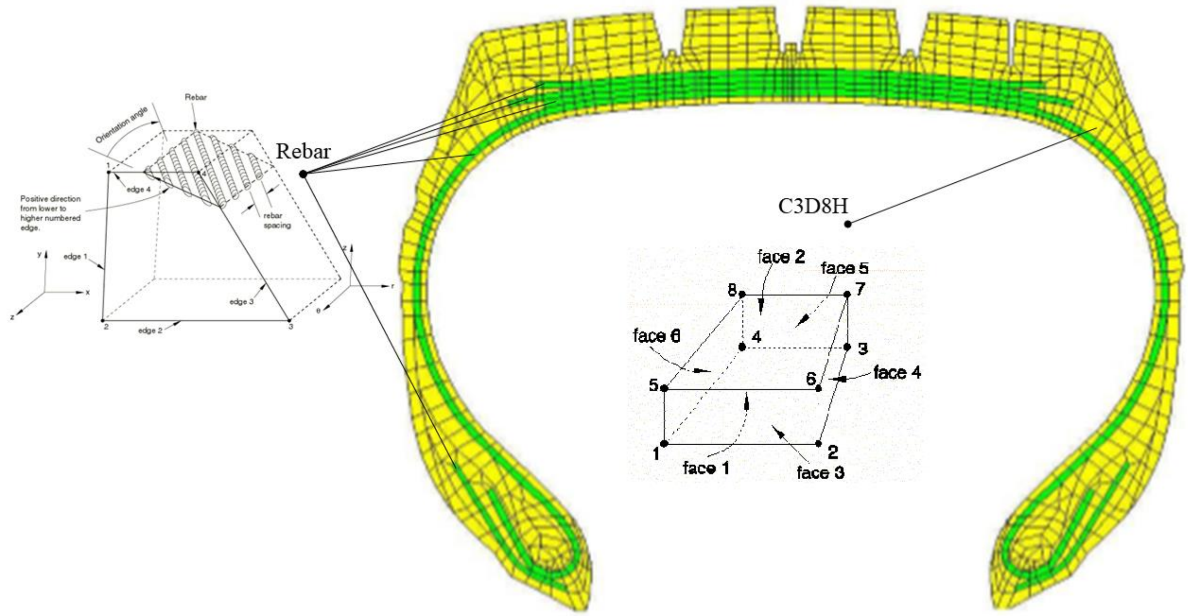

Figure 7. 3D finite element model with composites shown in green (Rebar) and rubber in yellow (C3D8H)

The cylindrical steel plunger with a hemispherical end was modeled according to Fig. 8.

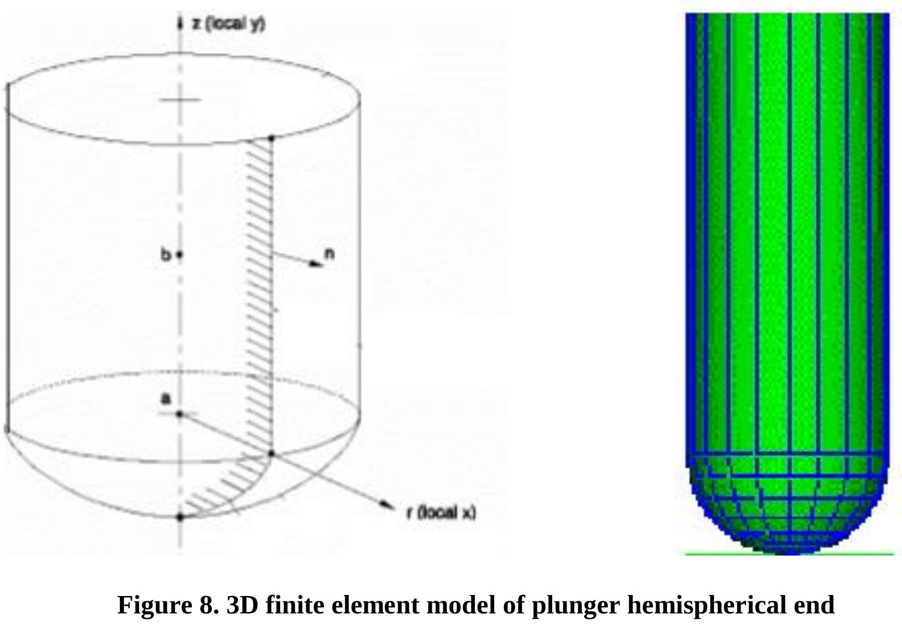

Figure 8. 3D finite element model of plunger hemispherical end

In order to validate the model response, tire experimental plunger test was performed and results were compared to simulation´s prediction. The comparison is depicted in Figs. 9 and 10.

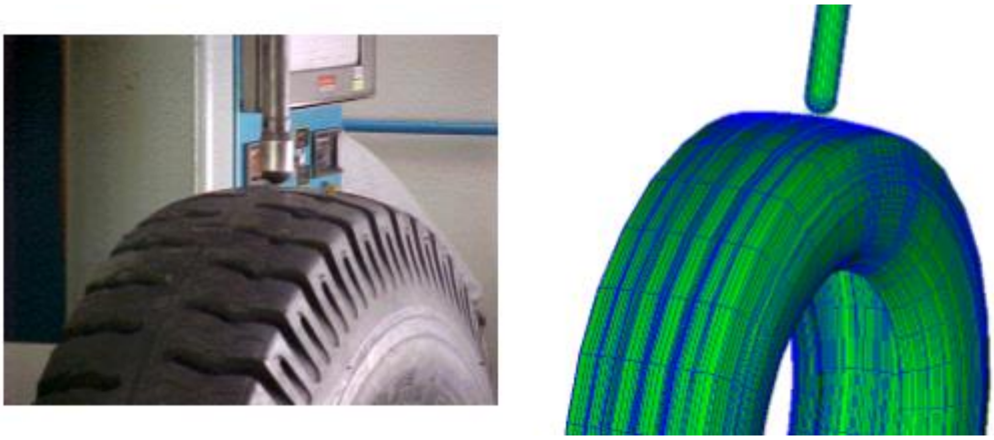

Figure 9. Plunger test vs model simulation

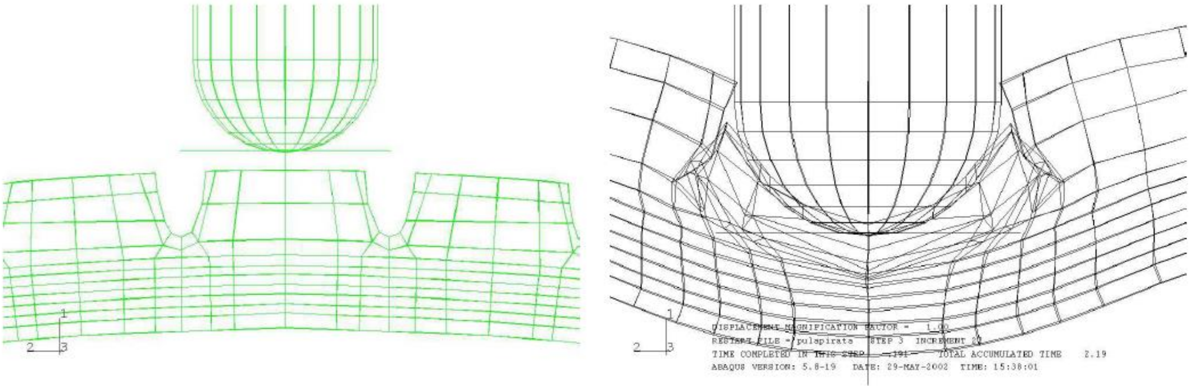

Figure 10. Tread deformation section

According to FMVSS No. 119 the minimum breaking energy strength to this specific truck tire size is 12500 lbf.in (1.14kJ). The standard specifies that each tire has to be tested in 5 spots. The test result should be considered as the average value. The plunger test performed had resulted in a 17701.5 lbf.in (2.0kJ), with a variation of 7% between the higher and the lower test result.

Tire simulation predicted a 15931.4 lbf.in (1.8 kJ), which represents a 9% difference between the tested tire and the model simulation. The results are depicted in Fig. 11.

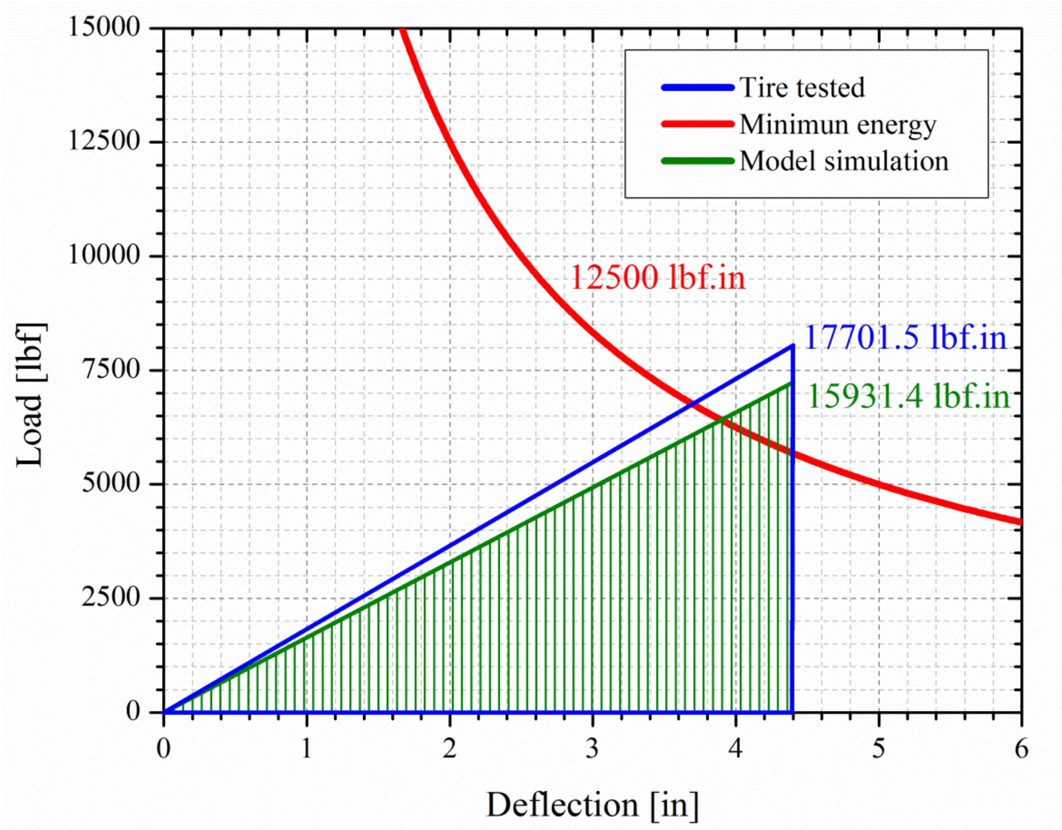

Figure 11. Plunger test vs model simulation results

6 CONCLUSIONS

The essential aspects of the elastomeric materials stress–strain behavior have been reviewed. The literature most frequently used models invariant-based and/or stretch-based continuum mechanics theories were explored.

Also the Halpin-Tsai model, that are used to describe tire composites, was approached. The equations represent empirical relationships that allow composites to be represented in terms of the matrix and reinforcing properties. The model curve is fitted to explicit exactly elastic solutions and endorsed by experimental measurements.

An investigation on the usage of hyperelastic constitutive model, calibrated with experimental data, to perform a finite element analysis on the response of tires subjected to plunger test, was described in detail in this article.

The proposed model can be used in design and/or optimization stages. By virtually reproducing the standards experimental procedures it is possible to reduce prototype production and testing. Far less prototype measurement is needed and hence the time-to-market and cost-to-market could be both significantly reduced.

According to Lee (2015), the quality of the tire models can be accessed via experimental validation measures or metrics. Comparisons between numerical and experimental plunger test results demonstrated the accuracy of the proposed model, with a 9% difference.

Numerical results showed that the model is arguably reliable and its convergence is fairly good.

Tires have a limited lifetime after which they are rendered unusable (Datta et al., 2017). It has been estimated that around 290 million tires are discarded annually in US (Brunet et al., 2016). So tire recycling became a major engineering concern (Machado et al., 2017; Czajczyńska et al., 2017; Bompa et al., 2017). According to Mangili et al. (2015) "scrap tire materials consume landfill space, spoil soil, groundwater and surface water. They also represent threats for public health and safety because of the risk for diseases and fires that may release toxic chemicals into the air". This is an important engineering and social matter that was not addressed in this article but must be considered in further studies in order to avoid environment damages (Derakhshan et al., 2017).

ACKNOWLEDGEMENTS

The authors acknowledge the financial support provided by CNPq (Conselho Nacional de Desenvolvimento Científico e Tecnológico), CAPES (Coordenação de Aperfeiçoamento de Pessoal de Nível Superior), FAPEMIG (Fundação de Amparo à Pesquisa do Estado de Minas Gerais) and UFMG (Universidade Federal de Minas Gerais). Also, they would like to express very great appreciation to peers of Pirelli Pneus S.A., CEA Poli-USP and Centro Universitário FEI for their valuable and constructive suggestions during the planning and development of this research work. Special thanks to Argemiro Luis de Aragão Costa, Ricardo Murilo Dias and Anderson Muniz Calhabeu.

REFERENCES

Abdolmaleki H., Jafari, A., Tabatabaeifar, A., Hajiahmad, A., & Goli, H., 2015. Development and evaluation of an in-situ tire testing facility with variable side slip angles. *Journal of Terramechanics, vol.* 59, pp. 49–58.

Abe, M., 2015. *Vehicle handling dynamics: theory and application*. Butterworth-Heinemann.

ASTM F414-06. 2006. Standard Test Method for Energy Absorbed by a Tire When Deformed by Slow-Moving Plunger, *ASTM International*, West Conshohocken, PA.

Baranowski, P., Malachowski, J., & Mazurkiewicz, L., 2016a. Numerical and experimental testing of vehicle tyre under impulse loading conditions. *International Journal of Mechanical Sciences*, vol. 106, pp. 346–356.

Behroozi, M., Olatunbosun, O.A., & Ding, W., 2012. Finite element analysis of aircraft tyre–Effect of model complexity on tyre performance characteristics. *Materials & Design*, vol. 35, pp. 810–819.

Bergstrom, J.S., 2015. *Mechanics of solid polymers: theory and computational modeling*. William Andrew.

Bompa, D.V., Elghazouli, A.Y., Xu, B., Stafford, P.J. & Ruiz-Teran, A.M., 2017. Experimental assessment and constitutive modelling of rubberised concrete materials. *Construction and Building Materials*, vol. 137, pp. 246–260.

Brunet, S., de la Llera, J.C. & Kausel, E., 2016. Non-linear modeling of seismic isolation systems made of recycled tire-rubber. *Soil Dynamics and Earthquake Engineering*, vol. 85, pp. 134–145.

Chang, C.L., & Yang, S.H., 2009. Simulation of wheel impact test using finite element method. *Engineering Failure Analysis*, vol. 16, pp. 1711–1719.

Chen, L., Chang, Z., & Qin, T., 2017. Elastic wave propagation in simple-sheared hyperelastic materials with different constitutive models. *International Journal of Solids and Structures*.

Cheviakov, A.F., & Ganghoffer, J.F., 2012. Symmetry properties of two-dimensional Ciarlet–Mooney–Rivlin constitutive models in nonlinear elastodynamics. *Journal of Mathematical Analysis and Applications*, vol. 396, pp. 625–639.

Cho, J., Lee, S., & Jeong, H.Y., 2015. Finite element analysis of a tire using an equivalent cord model. *Finite Elements in Analysis and Design*, vol. 105, pp 26–32.

Choi, S.H., & Lyu, M.Y., 2017. A study of rubber flow in a mold during the tire shaping process using experiment and computer simulation. *Polymer Testing, vol.* 61, pp. 258–268.

Costa, A.L.D.A., 2000. *Estudo de desgaste de pneus de caminhões e ônibus utilizando-se o Método dos Elementos Finitos.* Master´s degree thesis, University of São Paulo.

Costa, A.L.D.A., 2007. *Caracterização do comportamento vibracional do sistema pneu-suspensão e sua correlação com o desgaste irregular verificado em pneus dianteiros de veículos comerciais.* PhD thesis, University of São Paulo.

Cueto, O.G., Coronel, C.E.I., Morfa, C.A.R., Sosa, G.U., Gómez, L.H.H., Calderón, G.U. & Suárez, M.H., 2013. Three dimensional finite element model of soil compaction caused by agricultural tire traffic. *Computers and Electronics in Agriculture*, vol. 99, pp. 146–152.

Cueto, O.G., Coronel, C.E.I., Bravo, E.L., Morfa, C.A.R. & Suárez, M.H., 2016. Modelling in FEM the soil pressures distribution caused by a tyre on a Rhodic Ferralsol soil. *Journal of Terramechanics*, vol. 63, pp. 61–67.

Czajczyńska, D., Krzyżyńska, R., Jouhara, H. & Spencer, N., 2017. Use of pyrolytic gas from waste tire as a fuel: A review. *Energy*.

Dai Vu, T., Duhamel, D., Abbadi, Z., Yin, H.P. & Gaudin, A., 2017. A nonlinear circular ring model with rotating effects for tire vibrations. *Journal of Sound and Vibration*, vol. 388, pp. 245–271.

Datta, S., Antos, J. & Stocek, R., 2017. Characterisation of ground tyre rubber by using combination of FT-IR numerical parameter and DTG analysis to determine the composition of ternary rubber blend. *Polymer Testing*, vol. 59, pp. 308–315.

Derakhshan, Z., Ghaneian, M.T., Mahvi, A.H., Conti, G.O., Faramarzian, M., Dehghani, M., & Ferrante, M., 2017. A new recycling technique for the waste tires reuse. *Environmental Research*, vol. 158, pp. 462–469.

Diaz, C.G., Kindt, P., Middelberg, J., Vercammen, S., Thiry, C., Close, R., & Leyssens, J., 2016. Dynamic behaviour of a rolling tyre: Experimental and numerical analyses. *Journal of Sound and Vibration*, vol. 364, pp. 147–164.

Fiala, E., 1954. *Seitenkrafte am rollenden luftreifen'*Z. VDI bd. 96, no. 29.

Gillespie, T. D., 1992. *Fundamentals of Vehicle Dynamics*. Society of Automotive Engineers, Technology & Engineering - 495 pages.

Guiggiani, M., 2014. *The Science of Vehicle Dynamics*, DOI 10.1007/978-94-017-8533-4_2, © Springer Science+Business Media Dordrecht.

Gupta, V., & Narayanamurthy, G., Acharya, P., 2017. Can lean lead to green? Assessment of radial tyre manufacturing processes using system dynamics modelling. *Computers & Operations Research.*

Halpin, J.C., & Kardos, J.L., 1976. The Halpin-Tsai equations: a review. *Polymer Engineering & Science*, vol. 16, pp. 344–352.

Harris, J.R., & Evans, L.R., 2013. Evaluation of Laboratory Tire Tread and Sidewall Strength (Plunger Energy) Test Methods. *DOT Technical Report*. DOT HS 811 797.

Hoever, C. & Kropp, W., 2015. A model for investigating the influence of road surface texture and tyre tread pattern on rolling resistance. *Journal of Sound and Vibration*, vol. 351, pp. 161–176.

Jia, L.C., Li, Y.K., & Yan, D.X., 2017. Flexible and efficient electromagnetic interference shielding materials from ground tire rubber. *Carbon*, vol. 121, pp. 267–273.

Jones, N., 2003. Several phenomena in structural impact and structural crashworthiness. *European Journal of Mechanics-A/Solids*, vol. 22, pp. 693–707.

Kern, W.J., & Futamura, S., 1988. Effect of tread polymer structure on tyre performance. *Polymer*, vol. 29, pp. 1801–1806.

Kersker, T.M., Kovac, F.J., & Dague, M.F., 1969. The tire composite. *Fibre Science and Technology*, vol. 2, pp. 41–57.

Kuster, J., Jaureguizahar, L.F., Arechaga, T., 2013. Simulación de ensayo de energía de penetración de neumáticos basado en elementos finitos. *Mecánica Computacional*, vol XXXII, pp. 2453–2471. Argentine Association for Computational Mechanics (AMCA).

Khajehsaeid, H., Arghavani, J., Naghdabadi, R., & Sohrabpour, S., 2014. A visco-hyperelastic constitutive model for rubber-like materials: A rate-dependent relaxation time scheme. *International Journal of Engineering Science*, vol. 79, pp. 44–58.

Kim, H.H., Kim, D.G., Choi, J.Y., & Park, S.C., 2017. Tire mixing process scheduling using particle swarm optimization. *Computers & Industrial Engineering*, vol. 110, pp. 333–343.

Lee, J. H. 2015., Statistical modeling and comparison with experimental data of tire–soil interaction for combined longitudinal and lateral slip. *Journal of Terramechanics*, vol. 58, pp. 11–25.

Lijuan, L., Shenghua, S., & Lan, Z., 2014. Mechanical properties and constitutive equations of concrete containing a low volume of tire rubber particles. *Construction and Building Materials*, vol. 70, pp. 291–308.

Liu, F., Sutcliffe, M.P.F., & Graham, W.R., 2010. Prediction of tread block forces for a free-rolling tyre in contact with a smooth road. *Wear*, vol. 269, pp. 672–683.

Machado, S.L., Vilar, O.M., de Fátima Carvalho, M., & Karimpour-Fard, M., 2017. A constitutive framework to model the undrained loading of municipal solid waste. *Computers and Geotechnics*, vol. 85, pp. 207–219.

Maluf Filho, W.M., 2002. *Rudimentos da Mecânica dos Pneumáticos*. São Paulo. Master´s degree thesis, University of São Paulo.

Mangili, I., Lasagni, M., Anzano, M., Collina, E., Tatangelo, V., Franzetti, A., Caracino, P., & Isayev, A.I., 2015. Mechanical and rheological properties of natural rubber compounds containing devulcanized ground tire rubber from several methods. *Polymer Degradation and Stability*, vol. 121, pp. 369–377.

Marckmann, G., Chagnon, G., Le Saux, M., & Charrier, P., 2016. Experimental investigation and theoretical modelling of induced anisotropy during stress-softening of rubber. *International Journal of Solids and Structures*, vol. 97, pp. 554–565.

Matsubara, M., Tajiri, D., Ise, T. & Kawamura, S., 2017. Vibrational response analysis of tires using a three-dimensional flexible ring-based model. *Journal of Sound and Vibration*, vol. 408, pp. 368–382.

Montella, G., Calabrese, A., & Serino, G., 2014. Mechanical characterization of a Tire Derived Material: Experiments, hyperelastic modeling and numerical validation. *Construction and Building Materials*, vol. 66, pp. 336–347.

Mooney, M., 1940. A theory of large elastic deformation. *Journal of Applied Physics*, vol. 11, pp. 582–592.

Mouritz, A.P., & Gibson, A.G., 2007. *Fire properties of polymer composite materials*, vol. 143, Springer Science & Business Media.

Mullins, L., 1969. Softening of Rubber by Deformation. *Rubber Chemistry and Technology*, v. 42, p. 339–362.

Neves, R.R.V., Micheli, G.B., & Alves, M., 2010. An experimental and numerical investigation on tyre impact. *International Journal of Impact Engineering*, vol. 37, pp.685–693.

Ogden, R.W., 1972. Large deformation isotropic elasticity–on the correlation of theory and experiment for incompressible rubberlike solids. *Philosophical Transactions of the Royal Society of London A: Mathematical, Physical and Engineering Sciences*. vol. 326, no. 1567, pp. 565–584.

Ogden, R.W., 1997. *Non-linear elastic deformations*. Courier Corporation.

Ogden, R.W., 2007. Incremental statics and dynamics of pre-stressed elastic materials. *Courses and Lectures International Centre for Mechanical Sciences*, vol. 495, p.1.

Ozaki, S.,& Kondo, W., 2016. Finite element analysis of tire traveling performance using anisotropic frictional interaction model. *Journal of Terramechanics*, vol. 64, pp. 1–9.

Pavarini, E., van den Brink, J., Koch, E., & Sawatzky, G., 2016. *Quantum Materials: Experiments and Theory* (No. FZJ-2016-05129). Theoretische Nanoelektronik.

Rafei, M., Ghoreishy, M.H.R., & Naderi, G., 2017. Thermo-mechanical coupled finite element simulation of tire cornering characteristics—Effect of complex material models and friction law. *Mathematics and Computers in Simulation*.

Recuero, A., Serban, R., Peterson, B., Sugiyama, H., Jayakumar, P., & Negrut, D., 2017. A high-fidelity approach for vehicle mobility simulation: Nonlinear finite element tires operating on granular material. *Journal of Terramechanics, vol.* 72, pp. 39–54.

Rivlin, R.S., 1948. Large elastic deformations of isotropic materials. IV. Further developments of the general theory. *Philosophical Transactions of the Royal Society of London A: Mathematical, Physical and Engineering Sciences*, vol. 241, pp. 379–397.

Ružinskas, A., & Sivilevičius, H., 2017. Magic Formula Tyre Model Application for a Tyre-Ice Interaction. *Procedia Engineering*, vol. 187, pp. 335–341.

Sasso, M., Palmieri, G., Chiappini, G., & Amodio, D., 2008. Characterization of hyperelastic rubber-like materials by biaxial and uniaxial stretching tests based on optical methods. *Polymer Testing*, vol. 27, pp. 995–1004.

Schön, C.G., Angelo, C.M. & Machado, F.A.C., 2014. The role of tire size over the fatigue damage accumulation in vehicle bodies. *Procedia Materials Science*, vol. 3, pp. 331–336.

Shokrieh, M.M., & Moshrefzadeh-Sani, H., 2016. On the constant parameters of Halpin-Tsai equation. *Polymer*, vol. 106, pp. 14–20.

Simulia. *Abaqus analysis user's manual*, Version 6.13, Dassault Systems, 2016.

Sun, F., Hou, Y., Wang, L., Huang, L., & Qian, Z., 2017. A molecular dynamics (MD) simulation on tire-aggregate friction. *International Journal of Pavement Research and Technology*, vol. 10, n. 4, pp. 343–351.

Soares, R.M., & Gonçalves, P.B., 2014. Large-amplitude nonlinear vibrations of a Mooney–Rivlin rectangular membrane. *Journal of Sound and Vibration*, vol. 333, pp. 2920–2935.

Tang, T., Johnson, D., Smith, R.E., & Felicelli, S.D., 2014. Numerical evaluation of the temperature field of steady-state rolling tires. *Applied Mathematical Modelling*, vol. 38, pp. 1622–1637.

Tonatto, M.L., Forte, M.M. & Amico, S.C., 2017. Compressive-tensile fatigue behavior of cords/rubber composites. *Polymer Testing*, vol. 61, pp. 185–190.

Wang, R. & Wang, J., 2013. Tire–road friction coefficient and tire cornering stiffness estimation based on longitudinal tire force difference generation. *Control Engineering Practice*, vol. 21, pp. 65–75.

Wei, C., & Olatunbosun, O. A., 2016. The effects of tyre material and structure properties on relaxation length using finite element method. *Materials & Design*, vol. 102, pp. 14–20.

Winroth, J., Kropp, W., Hoever, C., & Hostmad, P., 2017. Contact stiffness considerations when simulating tyre/road noise. *Journal of Sound and Vibration*, vol. 409, pp. 274–286.

Wong, J.Y., 2008. *Theory of ground vehicles*. John Wiley & Sons.

Xia, K., 2011. Finite element modeling of tire/terrain interaction: Application to predicting soil compaction and tire mobility. *Journal of Terramechanic*s, vol. 48, pp. 113–123.

Xie, M., Tang, H. & Yao, H., 2016. Failure analysis of tire separation in two-sized tires on Airbus planes. *Engineering Failure Analysis*, 61, pp. 21–27.

Xiong, Y., & Tuononen, A., 2015. Rolling deformation of truck tires: Measurement and analysis using a tire sensing approach. *Journal of Terramechanics*, vol. 61, pp. 33–42.

Yeoh, O.H., 1993. Some forms of the strain energy function for rubber. *Rubber Chemistry and Technology*, vol. 66, pp. 754–771.

Zhao, C.L., & Zang, M.Y., 2017. Application of the FEM/DEM and alternately moving road method to the simulation of tire-sand interactions. *Journal of Terramechanics,* vol.72, pp. 27–38.